

Machine-Learning-Based Diagnosis of an Inverter-Fed Induction Motor

Bilal Djamal Eddine Cherif, Mohamed Chouai, Sara Seninete and Azeddine Bendiabdellah

Abstract—The principal objective of this paper is to detect and automatically monitor switch open-circuit faults in a two-level three-phase voltage source inverter fed induction motor from the processing of its current signals. The proposed diagnostic method uses both signal processing techniques and machine learning techniques in order to detect and localize the switch under an open-circuit fault. First, the Hilbert-Huang transform using the empirical ensemble mode decomposition is employed for each phase current signal, which leads to extracting the intrinsic mode functions. In order to optimally choose the function indicating the open-circuit fault harmonic, two factors, namely, the root mean square and the correlation coefficient are calculated out for each function. In this regard, two criteria are proposed that lead to choose the optimal function giving better information about the defected phase. The spectral envelope of the optimal function permits extracting the fault harmonic of the switch. Second, different machine learning techniques are applied to locate and classify the switch open-circuit faults with the hyper-parameters optimization for a better design of the different models. Finally, a comparative study of the different machine learning techniques is carried out for determining the best classifier for the open-circuit faults. The experimental results effectively demonstrate a very high classification rate of 98.98%.

Index Terms— CC, EEMD, IGBT, Inverter, Machine learning, Open-circuit fault, RMS, Spectral envelope.

I. INTRODUCTION

Currently, electric drives (three-phase power supply, Rectifier, inverter, induction motor and load) are considered the most used electromechanical conversion tools in the industrial field. Because this type of drive is justified by the simplicity of construction, with an optimal cost of repair and purchase of spare parts, as well as its mechanical robustness [1, 2].

Static converters, in particular inverters, are predominantly present in variable-speed electric drive systems. The reliability data from the literature justifies the field of application envisaged for the implementation of fault tolerance.

B. Djamal Eddine Cherif, Department of Electrical Engineering, Faculty of Technology, University of M'sila, M'sila 28000, Algeria. (e-mail: cherif.bilaldjamaledine@univ-msila.dz).

M. Chouai, Electrical Engineering Department, Faculty of science and Technology, University Abdelhamid Ibn Badis Mostaganem, Mostaganem 27000, Algeria, (e-mail: mohamed.chouai@univ-mosta.dz).

S. Seninete, Electrical Engineering Department, Faculty of Science and Technology, University Abdelhamid Ibn Badis Mostaganem, Mostaganem 27000, Algeria, (e-mail: sara.seninete@univ-mosta.dz).

A. Bendiabdellah, is with the Diagnosis Group, Laboratory of Electrical Drives Development (LDEE), Department of Electrical Engineering, University of Sciences and Technology of Oran Mohamed Boudiaf (USTO-MB), Algeria, (e-mail: bendiaz@yahoofr).

The percentage distribution of faults in an inverter is: 60% DC-link short-circuit fault, 31% Insulated-Gate Bipolar Transistor (IGBT) switch fault, and 6% diode fault [3].

A fault diagnosis is necessary to determine as precisely as possible the equipment to be repaired. The diagnosis should be carried out efficiently and has to permit early fault detection. This contributes to obtaining a better gain in productivity. Therefore, diagnosis becomes an integral part of the maintenance function [4, 5].

Several researchers have identified and developed various signal processing techniques allowing the detection and diagnosis of the IGBT switch open-circuit fault. Typical techniques include spectral analysis (Fast Fourier Transform) and time-frequency analysis (Short-Term Fourier Transform). Other more recent techniques allow better diagnosis of open-circuit fault; in particular, multi-resolution wavelet analysis and Hilbert-Huang transform (HHT) [6, 7].

HHT is a time-frequency analysis technique first introduced in 1998 by Huang. The principle of this technique is to adaptively decompose a signal into a sum of oscillating components, which has a single frequency to each sample. This operation is called empirical mode decomposition. It calculates the instantaneous frequency and the amplitude of its components using the Hilbert transform [8, 9 and 10]. Thus, signal processing techniques can only detect the faults without any information about its localization.

For enhancing the diagnosis, the detection of the fault should be accompanied by its localization. This allows automatic learning using the features extracted from the signal processed for a better classification of the open-circuit faults. This can be effectively done by the machine learning (ML) technology. Some of the common ML techniques are: Support Vector Machine (SVM), Naive Bayes (NB), K-Nearest Neighbors (KNN), Multi-layer Perceptions (MLP), and Random Forest (RF) [11]. A Support Vector Machine is a supervised ML algorithm that can be used for classification and regression purposes. SVMs are based on the idea of finding a hyper-plane that best divides the data into two classes [12].

The KNN algorithm is a nonparametric method that, serves for classification and regression. In both cases, it is a question of classifying the entry in the category to which belongs the k nearest neighbors in the space of the features identified by learning [13].

The NB classification is a type of simple probabilistic Bayesian classification based on Bayes' theorem with a strong (called naive) independence of assumptions. It implements a

naive Bayesian classifier. The NB belongs to the linear classifiers family [14].

The MLP is a type of artificial neural network organized in several layers within which information flows from the input layer to the output layer only; it is, therefore, a direct propagation network [15].

The RF is a classification algorithm that reduces the variance of forecasts from a single decision tree [16], thereby improving their performance. It combines many decision trees in a bagging-type approach [17].

In Supervised Learning, an ML algorithm will find a prediction/approximation function F , which will be based on predictive variables X and will approach a target variable Y such as $F(X) = Y$. One of the important aspects to consider in this function is: How will it generalize on data that it has not yet "seen" during the learning phase? This question is important because the goal of ML is to predict results on data not seen by the predictive function. The application goal is for the prediction made to be as close as possible to reality and this is after the model has trained on training data (Training Set). Indeed, when a Supervised Learning algorithm produces a prediction function/model F , it will be based on learning data. The function F produced will capture all the properties and correlations present in the Training Set. These properties and correlations are specific to the Training Set. This is why the learning data must be sufficiently representative of the problem studied, for better correlations captured by the predictive model. Consequently, the prediction model calculated at the end of the learning phase will be better generalizable and will allow more precise predictions on data that is not present in the Training Set. Two problems can occur during this operation: Overfitting and Underfitting. They are the main causes of the poor performance of predictive models generated by ML algorithms. First, Overfitting is a model that is too specialized on Training Set data and which will not be generalized. Second, Underfitting is a generalist model unable to provide precise predictions [18, 19].

The goal is to look for models that are in the "golden point". They must not suffer from Underfitting or Overfitting. Finding this "golden point" is the challenge in the field of data scientists. In fact, there are more sophisticated methods to find this point that gives the best performance. Among these methods, the hyper-parameters optimization of the methods used is applied in this paperwork.

II. RELATED WORKS

It is practically interesting to discuss the relevant work about the introduction of different signal processing and ML techniques for detecting several faults.

In [20], the authors focused on detecting and localizing open-circuit faults in a three-phase inverter supplying an induction motor. The authors carried out a comparative study between three detection techniques: the current drop measurement method, the average value of the currents method, and the Park vector method. The comparison evaluates each technique regarding the speed of detection, the performance and the

localization capacity. The simulation obtained and the experimental results clearly illustrate the detection efficiency of the current drop method based on the merits of the comparison study. On the other hand, these methods represent some limitations in terms of their inability to locate the failing IGBT, hence, it is used only for detecting failing legs. The second constraint is related to the hardware aspect given the fact that this technique uses six current sensors at each trigger of the six IGBTs of the three-phase two-level voltage inverter.

For the improvement of the diagnosis evaluation process of inverter open-circuit faults in synchronous motors, the authors in [21] discuss a diagnostic method based on current residuals and ML models. Instead of evaluating residues against thresholds, this technique is used to publish a full evaluation of current residues resulting from an observer state. To simplify the diagnostic process, machine-learning models simultaneously perform diagnosis and fault localization. In addition, the proposed scheme is implemented online. However, this online method needs a sampling strategy in order to reduce the big data amount taking a long time of calculation.

The authors in [22] propose a fault diagnosis technique using the least squares support vector machine with gradient information in order to repair IGBT open-circuit fault occurring inverters. They used the space vector transform to represent the inverter voltage scalar as a composite quantity to restrict fault signal redundancy and data processing capabilities. This technique diagnoses and identifies the characteristic vector of the voltage fault signal in an overly comprehensive dictionary. This technique has reached an accuracy of 98.92% for open-circuit IGBT fault diagnosis. Though, the lack of training data makes the regression quality poor. This restricts the SVM model generalization ability while losing its sparseness.

In [23], the authors studied various faults occurring in the electronic power circuit of an industrial drive. In addition, they presented the effect of various defects on the performance of the induction motor. Therefore, they proposed a real-time monitoring platform for detecting and classifying faults with accuracy based on ML. A diagnostic tool is then developed to reveal the localization of the fault as well as its severity to the operator in order to make corrective decisions. But the process takes long computation time due to the large data volume.

In [24], the authors planned to extract and identify fault features in power electronic circuits without supervision. They put forward a fault diagnosis technique using ML-based on sparse auto encoder and Broad learning system. On the one hand, simulation results of the thyristor fault diagnosis show that the technique performs better than traditional techniques. On the other hand, the method performance is low in terms of the accuracy when the signal is affected by noise bigger than 30 dB.

Our first contribution in this paperwork consists of applying Hilbert-Huang transform to decide about the IGBT inverter state. A recently proposed technique HHT, based on the Empirical Ensemble Mode Decomposition (EEMD) is used. This decomposition avoids the big data amount processing. A

specific test rig is realized to acquire real-time currents in both healthy and faulty cases. The diagnosis depends on the open-circuit fault harmonic presence.

The next contribution of this work consists in proposing an automatic localization and classification of the open-circuit fault of the IGBT switch of the inverter using the ML approach based on the features extracted from the HHT-EEMD technique. As a third contribution, ML techniques including SVM, KNN, NB, MLP, and RF are used and compared to define the best technique for the correct classification of this type of fault. The evaluation criteria used to measure the performance of the various proposed techniques are: accuracy, sensitivity, specificity, precision, g-mean, and calculation time.

The rest of this paper is organized as follows: In Section III, the HHT-based EEMD technique, and its algorithm are described. Section IV introduces the statistical study, which is used to optimally select the Intrinsic Mode Function (IMF) containing the frequencies characterizing the faults. This selection is based on two proposed criteria in terms of the Root Mean Square (RMS) and the Correlation Coefficient (CC). In Section V, the spectral envelope is presented. In Section VI, each ML technique and its algorithm are discussed in detail. The benchmarking study and the evaluation criteria are presented in Section VII. Furthermore, Section VIII discusses the experimental results, including the complete current acquisition chain and flowchart. In Section IX, comparative experimental results between different ML techniques are provided, giving details on the classification of open-circuit faults. Finally, Section X closes the article with conclusions and future work.

III. HILBERT-HUANG TRANSFORMS (HHT-EEMD)

This technique is used to extract the open-circuit fault of IGBT features by employing empirical ensemble mode decomposition [25, 26].

A. EEMD Algorithm

Step 01: Generate $x^{(i)} = x + \zeta \omega_n^{(i)}$ where $\omega_n^{(i)}$ ($i=1, \dots, I$) is a realization of white noise with zero mean unit variance, and standard deviation of noise $\zeta > 0$.

Step 02: Perform the decomposition of the signal $x^{(i)}$ for the modes $IMF_k^{(i)}$.

Step 03: The final IMF_s are the sets averages of the previous IMF_s .

$$IMF_k = \frac{1}{I} \sum_{i=1}^I IMF_k^{(i)} \quad (1)$$

IV. STATISTICAL STUDY

For the statistical study, two factors are used, notably, the root mean square and the correlation coefficient.

A. RMS

The effective value is a very characteristic value allowing measuring the average energy of the signal. It is used to detect abnormally high energy dissipations accompanying the birth of a fault [27]:

$$RMS = \sqrt{\frac{\sum_{i=1}^N (IMF(i))^2}{N}} \quad (2)$$

B. CC

The correlation coefficient between the stator current signals and IMF_i extracted using EEMD is given by the following equation [28]:

$$CC(i) = \frac{\sum_{t=1}^N \frac{x(t)IMF_i(t)}{\left(\sqrt{\sum_{t=1}^N x^2(t)} \sqrt{\sum_{t=1}^N IMF_i^2(t)} \right)}, \quad (3)$$

V. SPECTRAL ENVELOPE

Several consecutive treatments of the time signal are required to reach the spectral envelope. These are summarized in the following steps:

Step 01: Filtering the signal to eliminate insignificant components;

Step 02: Applying the Hilbert transform to calculate the envelope;

Step 03: The envelope spectrum is calculated, which gives information about the fault.

The spectral envelope is defined by the following equations [29]:

$$\overline{IMF}_i = \frac{1}{\pi} \int \left(\frac{IMF_i(\tau)}{t - \tau} \right) dt \quad (4)$$

$$\overline{IMF}_i = IMF_i(t) + j \overline{IMF}_i(t) \quad (5)$$

$$|\overline{IMF}_i(t)| = \sqrt{IMF_i(t)^2 + \overline{IMF}_i(t)^2} \quad (6)$$

VI. TECHNIQUES OF MACHINE LEARNING

For the localization and classification of the faulty IGBT, five techniques based on ML are proposed in this paper as follows: Support vector machines, K-nearest neighbors, Naïve bays, Multi-layer perceptron, and Random forests. Optimization of the hyper-parameters using hold-out validation is required to ensure the best performance. These parameters are the number of neurons of MLP, the number of trees of RF, the neighborhood number K of KNN, and those concerning the parameter of the polynomial kernel used in the SVM network.

A. Support Vector Machine (SVM)

This classification algorithm is given as follows [30, 31].

Step 01: The SVM Classifier construction:

For each input value x in a set R^d , a function f is constructed, which will correspond to an output value $y \in \{-1, 1\}$. The data space is changed with another one larger in dimension, using the nonlinear mapping function Φ . The learning function f in both linear and non-linear cases is described by the following model.

$$f(x) = \begin{cases} \text{if the problem is linear separable} \\ \text{sign}(\langle \omega_{c,C(c)} - x \rangle + b_{c,C(c)}) \\ \text{Else} \\ \text{sign}(\langle \omega_{c,C(c)} - \phi(x) \rangle + b_{c,C(c)}) \\ \text{End} \end{cases} \quad (7)$$

Step 02: The Hyper-Plane determination:

In the new spatial data, many hyper-planes separate, where maximizing the margin between the supporting vectors and its location, is the best. In order to establish the parameters of the function f , the optimal hyper-plane resulting from linear programming is described in the following model.

$$f(x) = \begin{cases} \text{if the problem is linear separable} \\ \text{sign} \left(\alpha_{c,C(c)}^T Xx + \frac{1}{y_i} (1 - \alpha_{c,C(c)}) \left(DKD + \frac{1}{j} I' \right) \right) \\ \text{Else} \\ \text{sign} \left(K(x, x^T) D \alpha_{c,C(c)} + \frac{1}{y_i} \left(1 - \alpha_{c,C(c)} \left(DKD + \frac{1}{j} I' \right) \right) \right) \\ \text{End} \end{cases} \quad (8)$$

For this study, a polynomial SVM (PSVM) has been used, in which his kernel (KR) is described by the following expression:

$$KR(x, x') = (1 + \langle x, x' \rangle)^p \quad (9)$$

Where: x and x' are vectors in the input space, p is the parameter to be optimized for the SVM with the polynomial kernel.

B. K-nearest neighbors (KNN)

This classification algorithm is given as follows [32, 33].

Step 01: Enter the D data sets. The training data set is defined by the following equation:

$$D = \{(X_i, Y_i), i = 1, \dots, N\} \quad (10)$$

Step 02: Define the distance function. The determination of the nearest neighbor is based on an arbitrary $(d(x, y))$ distance function is defined by the following equation:

$$d(X, Y) = \sqrt{\sum_{i=1}^N (X_i - Y_i)^2} \quad (11)$$

Step 03: Choose an integer of, K , K_r , either the number of observations from the group of nearest neighbors membership to the class r :

$$\sum_{r=1}^c K_r = K \quad (12)$$

Step 04: Calculate all the distances between the input observation and the other observations in the dataset.

Step 05: Keep the k observations of the dataset that are the "closest" to the observation to be predicted.

Step 06: Take the values y of K retained observations:

- For a regression, calculate the mean (or average) of y restraint.
- As for classification, calculate the y restraint form.

Step 07: Consider the value calculated in step 06 as the value that KNN predicted for the observation X .

C. Naïve Bayes (NB)

This classification algorithm is given by the following steps [34, 35].

Step 01: Determine the learning set.

Step 02: Determine the probability a priori in each class.

Step 03: Apply the function of Bayes:

$$P(Y = c / X = x) = \frac{P(X = x / Y = c)P(Y = c)}{P(X = x)} \quad (13)$$

To obtain the posterior probability of the classes at the point x .

Step 04: Choose the most probable class. In the formula of Bayes:

$P(Y = c)$: The a priori probability.

$P(X = x / Y = c)$: The conditional probability of membership to the class c , which can be interpreted as the verisimilitude of this class.

The prediction of naïve Bayesian classification can result in a case of equality where several classes obtain the same probability $P(Y)$.

Two approaches are proposed to handle these cases:

- Random choice: Randomly choose a class from the set of classes with the same probability $P(Y)$.
- Smallest index: Choose the first class encountered in all the classes with the same probability $P(Y)$.

D. Multilayer Perceptron (MLP)

This classification algorithm is given by the following steps [36, 37].

Step 01: Present a pattern of training to the network.

Step 02: Compare the network output to the output target.

Step 03: Calculate the error output of each network neurons.

Step 04: Calculate for each of the neurons, the output value that would have been correct.

Step 05: Define the increase or decrease necessary to obtain this local error value.

Step 06: Adjust for each connection, the weight to the lowest local error.

Step 07: Assign a correction to all previous neurons.

Step 08: Repeat from step 04 until reaching a performance threshold.

• **Learning**

Calculation of the mean squared error (MSE) defined by the following equation:

$$MSE(e_i, y_i) = \frac{1}{N} \sum_{i=0}^N (y_i - e_i)^2 \quad (14)$$

The mean absolute error (MAE) defined by the following equation:

$$MAE(e_i, y_i) = \frac{1}{N} \sum_{i=0}^N |y_i - e_i| \quad (15)$$

• **Calculation of the gradient**

The gradient ∇ is used to calculate the variation of the objective function with respect to any of the setting $\theta_{i,j}$.

$$\nabla C = \frac{\partial C}{\partial \theta_{i,j}} \quad (16)$$

Using the theorem derivation of the compound function, the variation of the objective function with respect to one of the weights is:

$$\nabla C = \frac{\partial C}{\partial \omega} = \frac{\partial C}{\partial \omega} \frac{\partial y}{\partial o} \frac{\partial C}{\partial y} \quad (17)$$

With $\frac{\partial y}{\partial o}$ the partial derivative of the activation function and $\frac{\partial C}{\partial y}$ the partial derivative of the objective function in regards to the final prediction y . By developing and using the rule of derivation of sums $\frac{d}{dx} \sum_i x_i = \sum_i \frac{d}{dx} x_i$:

$$\frac{\partial C}{\partial y_i} = \frac{\partial}{\partial y_i} \left(\frac{1}{N} \sum_{i=0}^N (y_i - e_i)^2 \right) = 2(y_i - e_i) \quad (18)$$

$\frac{\partial y}{\partial o} = y(1-y)$, if the function is sigmoid activation, or

$\frac{\partial y}{\partial o} = 1 - y^2$, the hyperbolic tangent:

$$\frac{\partial o}{\partial \omega} = y_{i-1} \quad (19)$$

E. Random Forests (RF)

This classification algorithm is given by the following steps [38].

Step 01: Select the random data points K from the training set.

Step 02: Construct the decision trees associated with the selected data points (subset).

Step 03: Choose the N number for the decision trees you want to create.

Step 04: Repeat steps 01 and 02.

Step 05: For new data points, search predictions of each decision tree and assign the new data points to the class that wins the majority votes.

VII. EVALUATION CRITERIA

The performance of data classification can be assessed in terms of:

A. Accuracy

The percentage of examples that are correctly classified is calculated according to [39]:

$$Acc = \frac{T_P + T_N}{T_P + T_N + F_P + F_N} \quad (20)$$

Where T_P : True positive; T_N : True negative; F_P : False positive and F_N : False negative.

B. Sensitivity

When the fault occurs, the ability to get a positive result is calculated according to [39]:

$$Sens = \frac{T_P}{T_P + F_N} \quad (21)$$

C. Specificity

Once the fault is absent, the ability of getting a negative result is calculated according to [39]:

$$Spec = \frac{T_N}{T_N + F_P} \quad (22)$$

D. Precision

It is the ratio of predicted positive examples which really are positive is defined as follow [39]:

$$Prec = \frac{T_P}{T_P + F_P} \quad (23)$$

E. G-mean

It is the geometric mean of sensitivity and precision [39] given a:

$$GSP = \sqrt{Sens \times Prec} \quad (24)$$

VIII. EXPERIMENTAL RESULTS AND DISCUSSION

A. Dataset Preparation

Experimental tests dealt with in this paperwork are carried out in our laboratory under the various IGBT switch faults occurring a two-level three-phase voltage source inverter. Each defect is characterized by a particular frequency, which appears in the current signals at specific harmonics. The inverter used is of the SEMIKRON type, controlled by a DSPACE 1104 card and supplying a three-phase induction motor coupled to a direct current generator (2.4 kW) forming the tests rig. The induction motor is of the AZZAZGA type, 50 (S/s), 4 poles, 3 Kw, with a stator current of 7 A. Fig.1 shows the real photo of the test rig and the structure of a three-phase voltage inverter.

The measuring system has three current sensors (FLUCK i30s, AC/DC CURRENT CLAMP), three voltage sensors (TEKTRONIX P5200) and DSPACE 1104 acquisition card. Finally, the whole set is connected to a computer for

visualizing the processed acquired signals. The acquisitions are acquired under a permanent state using a sampling frequency of 1500 (S/s) and acquisition time of 20s.

Five signal acquisitions (without noise, affected by a noise of 30db, 60db, 70db, and 90db) for the healthy and six faulty cases have been realized. While decomposing each signal with the EEMD giving 12 functions, the dataset widens to 420 signals. To train the ML techniques, the dataset is divided into a training set containing 80% (336 signals) of the data and a testing set containing 20% (84 signals) of the data.

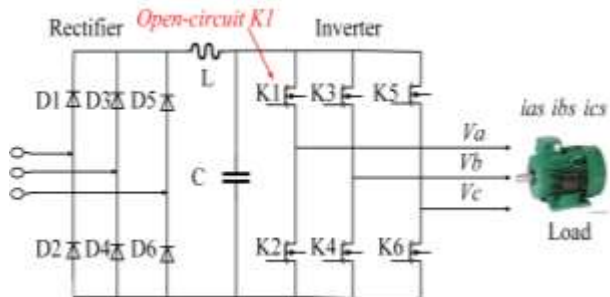


Fig. 1. The test rig and the structure of a three-phase voltage inverter.

The proposed diagnosis method is presented by the flowchart of Fig. 2.

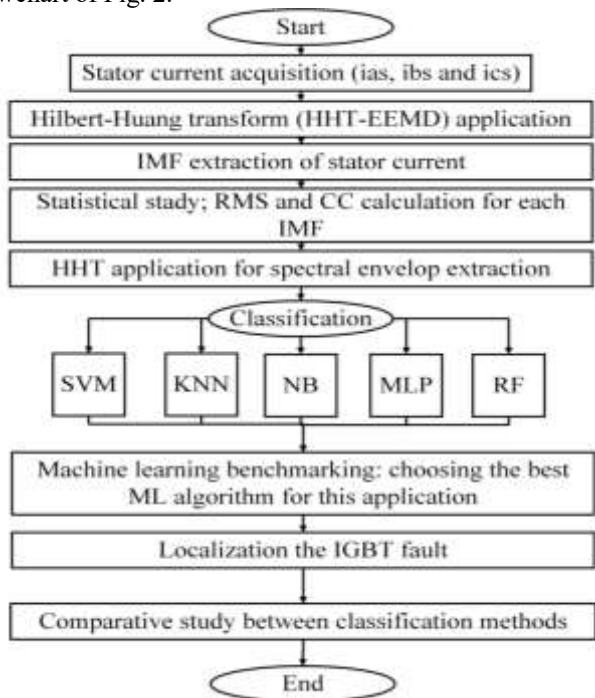


Fig. 2. Organization flowchart of the proposed diagnosis method.

Fig. 3 shows the stator current waveforms in both healthy inverter and faulty inverter under open-circuit fault in IGBT switch K_1 .

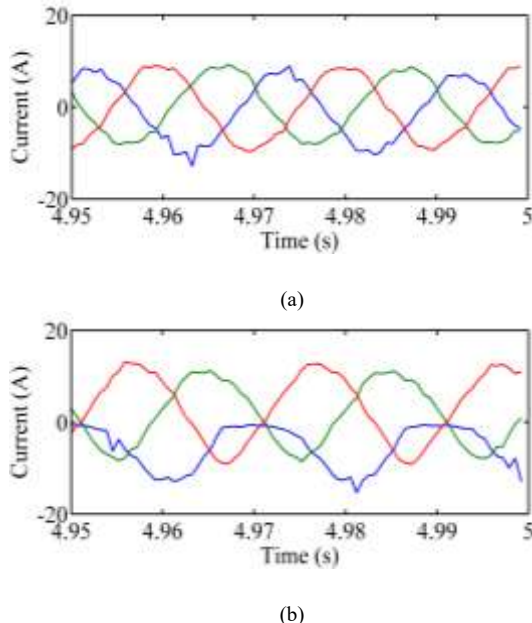


Fig. 3. Stator current. (a): Healthy case. (b): Open circuit at the IGBT switch K_1 .

Compared to the healthy case, the stator current in faulty case reveals a disappearance of the positive alternation of the stator current. The defective phase current is no longer controlled because it is only negative or zero. In these conditions; the sum of the other two healthy phases current is zero and take instantaneously high values.

B. Open-Circuit Fault Detection of An IGBTB based on Hilbert-Huang Transform (HHT-EEMD)

Table I, Shows the values of RMS and CC for inverter Healthy Case (HC) and inverter Open-Circuit faulty cases at different switches K_i of the IGBT (OCK $_i$).

TABLE I
VALUES OF RMS AND CC

| | | Phase A | | | | |
|----------|--------|----------|----------|---------------|---------|---------|
| Case | Factor | IMF_1 | IMF_2 | IMF_3 | IMF_4 | IMF_5 |
| HC | RMS | 251.9566 | 403.3936 | 61.0489 | 30.6489 | 9.0559 |
| | CC | 0,1046 | 0,6136 | 0,8859 | 0,0141 | -0,0125 |
| OCK $_1$ | RMS | 194.3855 | 301.4486 | 50.4821 | 25.4111 | 6.0956 |
| | CC | 0,1033 | 0,4503 | 0,5404 | 0,0109 | 0,0380 |
| OCK $_3$ | RMS | 300.6402 | 489.8179 | 80.4930 | 26.7508 | 1.1234 |
| | CC | 0,1133 | 0,6206 | 0,9086 | 0,0178 | 0,0022 |
| | | Phase B | | | | |
| HC | RMS | 223.6102 | 408.2912 | 90.4254 | 62.0695 | 58.3594 |
| | CC | 0,1035 | 0,6017 | 0,9294 | 0,0232 | 0,0128 |
| OCK $_1$ | RMS | 283.3852 | 439.9218 | 66.3609 | 31.2290 | 13.1800 |
| | CC | 0,1290 | 0,5849 | 0,8667 | 0,0183 | 0,0157 |
| OCK $_3$ | RMS | 181.0842 | 301.1311 | 50.1170 | 26.0780 | 2.6762 |
| | CC | 0,1084 | 0,4968 | 0,6687 | 0,0075 | 0,0941 |
| | | Phase C | | | | |
| HC | RMS | 255.5148 | 434.2296 | 71.0446 | 40.6477 | 18.9682 |
| | CC | 0,0721 | 0,6129 | 0,9200 | 0,0086 | 0,0003 |
| OCK $_1$ | RMS | 288.5511 | 495.9374 | 72.5269 | 42.8110 | 15.2353 |
| | CC | 0,1072 | 0,5505 | 0,8739 | 0,0169 | 0,0013 |
| OCK $_3$ | RMS | 278.6332 | 441.4813 | 65.2009 | 32.7633 | 11.3940 |
| | CC | 0,0701 | 0,5942 | 0,8774 | 0,0044 | 0,00072 |

When the open-circuit fault occurs at K_1 (OCK_1), the leg corresponding to phase A becomes defected. According to Table I, one can notice that, for each IMF, the RMS of phase A has the minimum value compared to phases B and C. This indicates the presence of the open-circuit fault at phase A. Likewise, once the switch K_3 is under open-circuit (OCK_3), the RMS value of phase B is the minimum value compared to the RMS values of the other phases. Thus, the faulty phase has always the minimum RMS value. Further information can be extracted from the IMF containing the useful information properly indicating the existence of the open-circuit fault of the IGBT's. Hence, the optimal IMF should reveal a strong relationship with the original current signal. This corresponds to a correlation coefficient value close to one. For all the healthy and faulty cases, Table I indicates that the IMF₃ represents the closest CC value to 1. Then, a spectral envelope must be performed for the IMF₃.

C. Spectral Envelope of IMF₃

Fig. 4 shows the spectral envelope of the IMF₃ of phase A in both healthy and faulty OCK_1 cases.

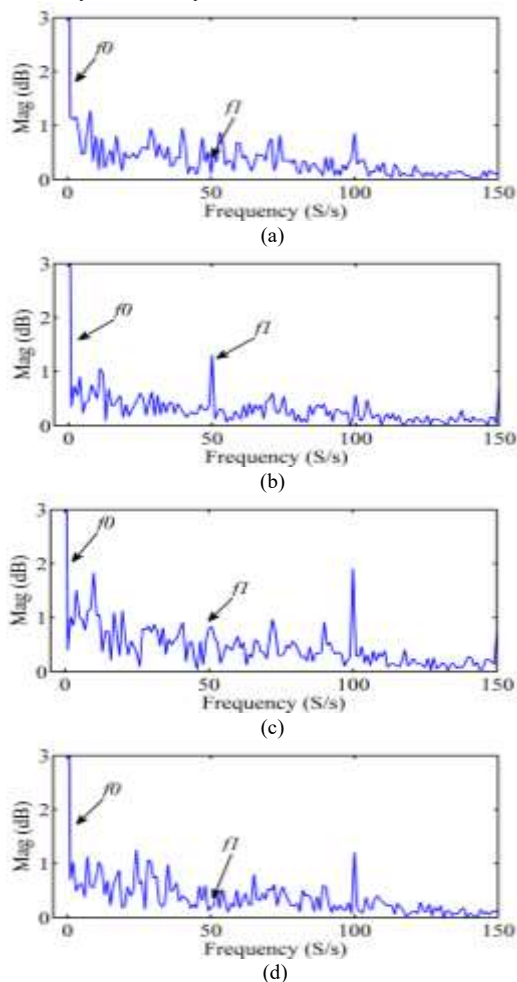


Fig. 4. Spectral envelope (a): HC. (b): IMF₃. (c): IMF₂. (d): IMF₅.

On the one hand, Fig.4.a, depicts the appearance of the DC component $f_0=0$ (S/s) and the frequency 100(S/s), while a no-fault signature emerges. On the other hand, in the presence of the open-circuit fault at the IGBT switch K_1 as illustrated

by the fig.4.b, the harmonic appears at $f_i=50$ (S/s). A comparative study of the spectral envelope between the healthy inverter and the faulty inverter (OCK_1), clearly shows a frequency signature around 50(S/s). This indicates that the frequency f_i is the frequency characterizing the IGBT switch open-circuit fault.

In order to validate while emphasizing the criteria used to choose the optimal IMF, fig.4 depicts the spectral envelope of IMF₂ and IMF₅ besides the IMF₃ of the faulty phase A when the switch K_1 is under open-circuit fault (OCK_1). The frequency characterizing the fault f_i does not appear clearly in the spectral envelope of IMF₂ and IMF₅. The IMF₃ displays f_i with the highest amplitude after the DC component f_0 .

Table II and Table III show respectively the amplitudes of the two harmonics (f_0 and f_i) for each case.

TABLE II
AMPLITUDES OF f_0

| Case | Phase A | Phase B | Phase C |
|---------|--------------|--------------|--------------|
| HC | 8.676 | 8.422 | 8.538 |
| OCK_1 | 7.509 | 9.402 | 9.361 |
| OCK_2 | 7.067 | 8.378 | 9.165 |
| OCK_3 | 10.6 | 7.061 | 9.887 |
| OCK_4 | 9.105 | 5.596 | 8.925 |
| OCK_5 | 9.172 | 9.584 | 7.209 |
| OCK_6 | 9.679 | 9.871 | 6.517 |

TABLE III
AMPLITUDES OF f_i

| Case | Phase A | Phase B | Phase C |
|---------|---------|---------|---------|
| HC | 0 | 0 | 0 |
| OCK_1 | 1.359 | 0 | 1.954 |
| OCK_2 | 1.444 | 0 | 1.593 |
| OCK_3 | 0 | 1.1079 | 0 |
| OCK_4 | 0 | 1.429 | 0 |
| OCK_5 | 1.545 | 0 | 1.368 |
| OCK_6 | 1.449 | 0 | 1.216 |

Similar to the RMS criteria, the presence of the fault is indicated in a phase once the amplitude of f_0 in this phase is minimal compared to the other phases.

Otherwise, f_i has amplitude of zero for all the phases in the healthy case. While in the faulty case of phase A (OCK_1 and OCK_2), f_i is of zero amplitude in phase B and has minimum amplitude in phase A compared to that of phase C. Similarly, if phase C is defected (OCK_5 and OCK_6), f_i is of zero amplitude in phase B, and has a minimum amplitude in phase C compared to that of phase A. Though, when phase B is under fault (OCK_3 and OCK_4), f_i has an amplitude of zero for the two others phases. Hence, in terms of this accordance, the frequencies f_i and f_0 are considered as features to train the different ML models.

D. Localization and Classification of Fault IGBT based on Machine Learning

Five ML techniques, namely the SVM, the KNN, the NB, the MLP and the RF, are employed to localize and classify the faulty IGBTs. By applying a benchmarking study on these

algorithms, the best technique is then chosen based on the best predictive performance.

The features used to train the models of ML are:

- RMS of each phase
- CC of each phase
- Amplitude of the frequency f_0 of each phase.
- Amplitude of the frequency f_1 of each phase.

Fig.5 shows the features used to train the ML models.

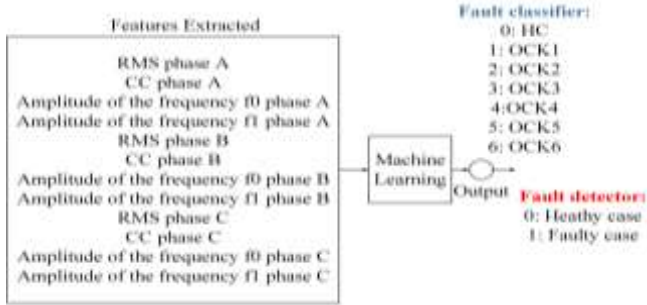
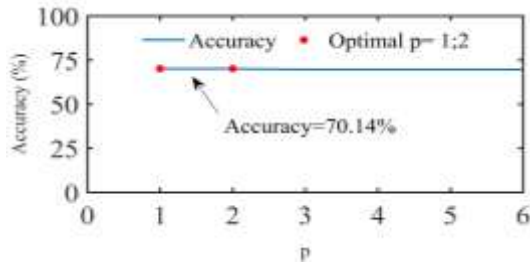


Fig. 5. Schematic diagram of a fault classifier based on machine learning.

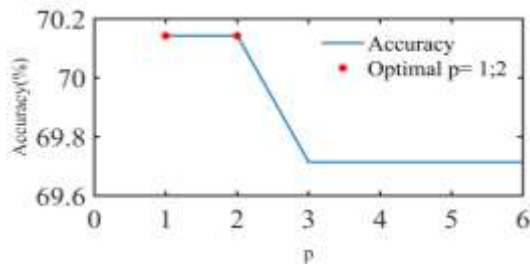
Hyper-parameters in ML methods are important because they directly control the behavior of the training algorithm and have a significant impact on the performance of the model being trained.

Optimization of the hyper-parameters using Grid-Search is required to ensure the best localization and classification of IGBT's fault. After the processing step (consisting of features extraction), the process of optimization is applied. These hyper-parameters are the number of neurons of MLP, the number of trees of RF, the neighborhood number K of KNN, and the SVM network. Note that there are no hyper-parameters to be optimized for NB and SVM (since the linear kernel is used).

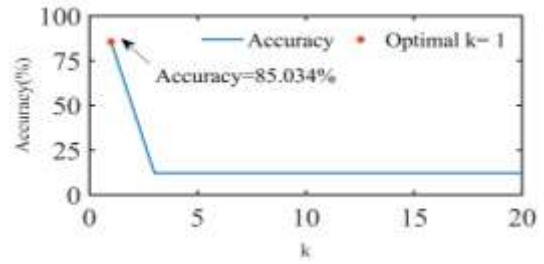
Fig. 6 shows the accuracy as a function of the (p , k , nodes number and trees number).



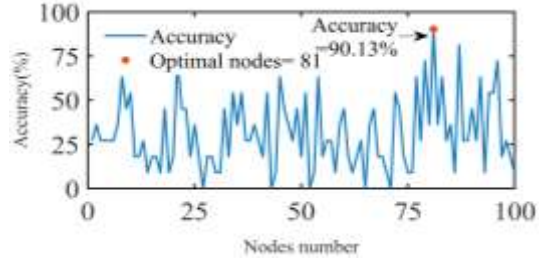
(a)



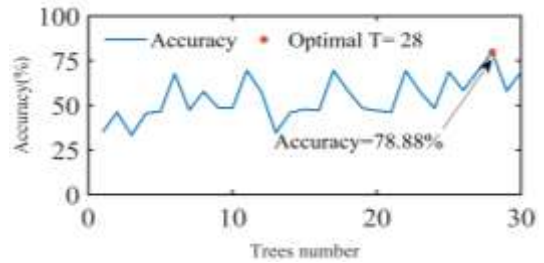
(b)



(c)



(d)



(e)

Fig. 6. Accuracy as a function (p , k , nodes number and trees number). (a): SVM. (b): Slice of SVM. (c): KNN. (d): MLP. (e): RF.

Fig.6a shows that overfitting occurs when the parameter p of the PSVM network exceeds 2 and underfitting occurs for a number below this value, which implies that this number is the optimal one. Similarly, Fig. 6a, 6c, 6d and 6e show that 1; 2, 1, 81, and 28 are the optimal values for the hyper-parameters of the KNN, MLP, and RF, respectively.

The choice of the appropriate hyper-parameters plays a crucial role in the success of the used algorithms. Since this choice has a huge impact on the learned model. Choosing good hyper-parameters offers two advantages [40]:

- Efficiently search the space of possible hyper-parameters
- Easy to manage a large number of experiments for tuning hyper-parameters.

From these results, it can be concluded that the introduction of classification techniques based on ML improves the efficiency of detection. The differences in how EEMD-based ML techniques work can be seen in the results shown in Fig. 6. The output of the EEMD based detector works well, as far as the expected value is concerned. This greatly increases the stability and the average accuracy of the detection, which is demonstrated in Fig. 7.

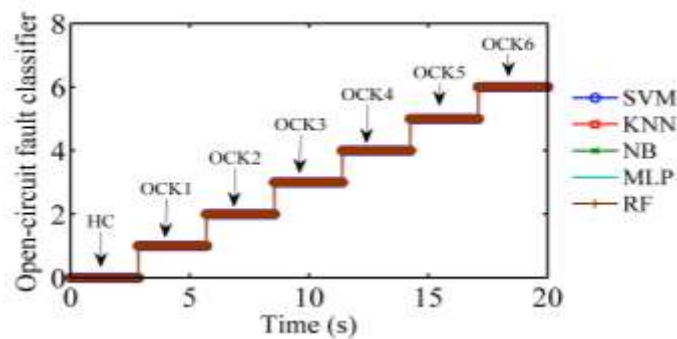


Fig. 7. Waveforms of output values from the different machine learning techniques-based fault classifiers.

IX. COMPARATIVE STUDY BETWEEN THE DIFFERENT MACHINE LEARNING TECHNIQUES PROPOSED

This comparison is made between the five techniques proposed previously in order to evaluate each one according to the evaluation criteria: the accuracy, the sensitivity, the specificity, the precision, the g-mean, and the calculation time. Table IV, summarizes the comparison between ML techniques. Fig.8 shows the evaluation criteria and the calculation time for each technique.

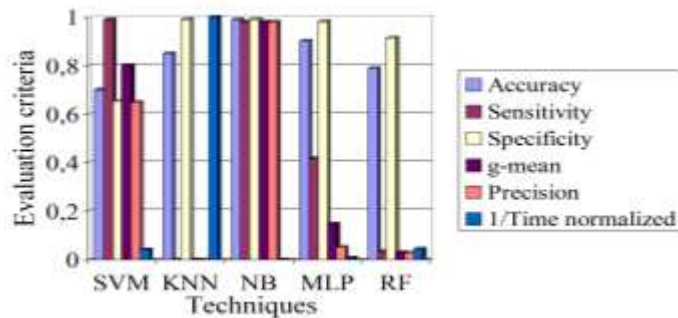


Fig. 8. Evaluation criteria and calculation time for each technique.

TABLE IV
COMPARISON BETWEEN MACHINE LEARNING TECHNIQUES

| Techniques | Accuracy | Sensitivity | Specificity | Precision | g-mean | 1/Time normalized |
|------------|-------------|--------------|-------------|-------------|-------------|-------------------|
| SVM | 0,7014 2 | 0,99 | 0,65333 | 0,6483 | 0,801 15 | 0,0411 |
| KNN | 0,8503 4 | 0 | 0,99206 | 0 | 0 | 1 |
| NB | 0,9898 | 0,97959 1 | 0,99149 | 0,9794 | 0,979 5 | 0,00001 |
| MLP | 0,9013 6 | 0,41666 6 | 0,98214 | 0,0510 1 | 0,145 8 | 0,0059 |
| RF | 0,7888 1 | 0,03260 | 0,91485 | 0,0270 5 | 0,029 7 | 0,0434 |

This comparative study clearly shows that the best technique in terms of precision, time calculation, g-mean and accuracy, is NB which takes in overall the best values of evaluation criteria. Despite its “naive” design model and the simple assumptions of the Naive Bayes algorithm, this method gave the best performance in this application. This is supported by other studies, such as [41], in which Chouai et al. applied a supervised machine learning study for the

detection/classification in an image processing field. The results obtained over their study confirm the same result herein. The main reason for the performance of NB is conditional independence. For detailed information, the authors recommend this article to understand the mathematical reasons [42]. Otherwise, the RF, MLP, and KNN respectively show a very low sensitivity and precision. Eventually, the SVM gives the lowest accuracy, while having poor specificity and precision. This leads to the fact that these algorithms have trouble predicting the negative class (the class which indicates the fault presence).

X. CONCLUSION

In this paper, a diagnostic method is presented to detect and automatically monitor the open-circuit fault of the IGBT switches occurring a two-level three-phase voltage source inverter fed induction motor. The proposed diagnostic uses as a first contribution, the HHT-EEMD to provide the IMF, which contains useful information about the open-circuit fault of the inverter IGBT switch. A statistical study based on the calculation of the RMS and the correlation coefficient is then carried out for each IMF in order to determine the best choice of the optimal IMF. The results obtained correspond fully to the RMS and CC conditions. Presenting the IMF₃ with its spectral envelope eases detecting the harmonic corresponding to the open-circuit fault of the IGBT switch. The second contribution of this work is to apply different ML techniques (SVM, KNN, NB, MLP, and RF) based on the features extracted from the HHT-EEMD. These techniques were optimized by fitting their hyper-parameters in order to automatically locate and classify the IGBT switch open-circuit faults. The third and final contribution consists of comparing the different ML techniques employed for fault monitoring in induction motors. The comparison is made based on different evaluation criteria notably accuracy, sensitivity, specificity, precision, g-mean, and time calculation for each technique. The Naïve Bays technique seems to be the conventional technique for the correct classification of this type of fault. The experimental results obtained using the proposed diagnostic method clearly demonstrate its effectiveness with a very high classification rate in particular for the Naïve Bays technique compared with other machine learning techniques.

The specification of the number of faults can be the next procedure of the research on ML-based fault diagnosis. Further extension of the work is being carried out for other types of inverter faults while other fault types of induction motors.

APPENDIX

IGBT: Bipolar isolated trigger transistor; **HHT**: Hilbert-Huang transforms; **EMD**: Empirical Mode Decomposition; **EEMD**: Ensemble Empirical Mode Decomposition; **IMF**: Intrinsic modal function; **SVM**: Support Vector Machine; **NB**: Naive Bayes; **KNN**: K-Nearest Neighbors; **MLP**: Multi-layer Perceptions; **RF**: Random Forest; **ML**: Machine Learning; **Acc**: Accuracy; **Sens**: Sensitivity;

Spec: Specificity; **GSP:** G-mean; **Prec:** Precision; **i_{as} :** Stator current of phase A; **i_{bs} :** Stator current of phase B; **i_{cs} :** Stator current of phase C; **I :** Sets number of iterations; **ω_n :** White noise; **ξ :** Noise standard deviation; **RMS:** Root mean square; **CC:** Correlation coefficient; **N:** Number of signal points; **IMF(i):** Instantaneous value of the IMF; **$x(t)$:** Stator current signal; **T_p :** True positive; **T_n :** True negative; **F_p :** False positive; **F_n :** False negative; **f_0 :** DC component frequency; **f_i :** Frequency which characterizes the open-circuit fault at the IGBT switch; **t :** Time variable; **τ :** Relaxation time; **f :** Linear function; **ω :** Weight vector; **α :** Lagrange multipliers; **C:** Class addition; **I :** Identity matrix; **j :** Tuning parameter for error accepted; **p :** Parameter to be optimized for the SVM with the polynomial kernel; **D:** Available dataset or learning sample; **K_r :** Number of observations from the closest neighbor group belonging to the class r ; **K:** Number of neighbors to consider; **OCHK:** Open-Circuit Fault at the IGBT switch K_i .

REFERENCES

- [1] N. Rajeswaran, M. Swarupa, T. RAO, and al, "Hybrid artificial intelligence based fault diagnosis of svpwm voltage source inverters for induction motor," *Materials Today: Proceedings.*, vol.5, no.1, pp. 565-571, 2018.
- [2] Xu, Huaqing, Yanqing Peng, and Lumei Su. "Research on Open Circuit Fault Diagnosis of Inverter Circuit Switching tube Based on Machine Learning Algorithm." *IOP Conference Series: Materials Science and Engineering*. Vol. 452. No. 4. IOP Publishing, 2018.
- [3] C. Bilal Djamel Eddine, B. Azeddine, and T. Mostefa, "Diagnosis of an Inverter IGBT Open-circuit Fault by Hilbert-Huang Transform Application." *Traitement Du Signal*, vol.36, no.2, pp.127-132, 2019.
- [4] F. Calabrese, A. Regattieri, M. Bortolini, M. Gamberi, and F. Pilati, "Predictive Maintenance: A Novel Framework for a Data-Driven, Semi-Supervised, and Partially Online Prognostic Health Management Application in Industries." *Applied Sciences*, vol. 11, no.8,pp.3380, 2021.
- [5] U. Izagirre, I. Andonegui, A. Egea, and U. Zurutuza, "A Methodology and Experimental Implementation for Industrial Robot Health Assessment via Torque Signature Analysis." *Applied Sciences*, vol.10,no.21,pp.7883, 2020.
- [6] C, Vincent, and M Benbouzid. "Induction machine diagnosis using stator current advanced signal processing." *International Journal on Energy Conversion*,vol.3, no.3, pp.76-87, 2015.
- [7] S. Sara, and al. "On the Use of High-resolution Time-frequency Distribution Based on a Polynomial Compact Support Kernel for Fault Detection in a Two-level Inverter." *Periodica Polytechnica Electrical Engineering and Computer Science*, vol.64, no.4, pp.352-365, 2020.
- [8] H. Guoqing, and al. "Time-frequency analysis of nonstationary process based on multivariate empirical mode decomposition." *Journal of Engineering Mechanics*, vol.142, no.1, pp. 04015065, 2016.
- [9] S, M. Mousavi, A, L. Charles. "Automatic noise-removal/signal-removal based on general cross-validation thresholding in synchrosqueezed domain and its application on earthquake data." *Geophysics*, vol.82, no.4, pp.211-227, 2017.
- [10] Y. Yang, Z. Peng, W. Zhang, & G. Meng. "Parameterised time-frequency analysis methods and their engineering applications: A review of recent advances." *Mechanical Systems and Signal Processing*, vol.119, pp. 182-221, 2019.
- [11] L. N. Gueye, J. M. Flaus, and O. Adrot. "Review of machine learning approaches in fault diagnosis applied to iot systems." *International Conference on Control, Automation and Diagnosis (ICCAD)*. IEEE, 2019.
- [12] S. Akash, S. Chowdhuri, and S. S. Williamson. "Machine Learning-Based Data-Driven Fault Detection/Diagnosis of Lithium-Ion Battery: A Critical Review." *Electronics*, vol.10, no.11, pp.1309, 2021.
- [13] S. Hassan, and A. Karamodin. "A novel anomaly detection method based on adaptive Mahalanobis-squared distance and one-class kNN rule for structural health monitoring under environmental effects." *Mechanical Systems and Signal Processing*, vol.140, pp.106495, 2020.
- [14] K. S. Mambwe and Y. Sun. "A deep learning method with wrapper based feature extraction for wireless intrusion detection system." *Computers & Security*, vol.92, pp.101752, 2020.
- [15] K. Georgios, E. P. Koumoulos, and C. A. Charitidis. "Classification of mechanism of reinforcement in the fiber-matrix interface: Application of Machine Learning on nanoindentation data." *Materials & Design*, vol.192, pp.108705, 2020.
- [16] Y. Freund, and L. Mason. "The alternating decision tree learning algorithm." *In icml*, vol.99, pp.124-133, 1999.
- [17] Y. Zhendong, and al. "A novel arc fault detection method integrated random forest, improved multi-scale permutation entropy and wavelet packet transform." *Electronics*, vol.8, no.4, pp.396, 2019.
- [18] F.Y. Osisanwo, J. E. T. Akinsola, O. Awodele, J. O. Hinmikaiye, O. Olakanmi and J. Akinjobi. "Supervised machine learning algorithms: classification and comparison." *International Journal of Computer Trends and Technology (IJCTT)*, vol.48, no.3, pp.128-138, 2017.
- [19] H. Jabber, and R. Z. Khan. "Methods to avoid over-fitting and under-fitting in supervised machine learning (comparative study)." *Computer Science, Communication and Instrumentation Devices*, pp.163-172.
- [20] C. Bilal Djamel Eddine and al. "A comparative study between methods of detection and localisation of open-circuit faults in a three phase voltage inverter fed induction motor." *International Journal of Modelling, Identification and Control*, vol.29, no.4, pp.327-340, 2018.
- [21] Z. Zeliang, and al. "A hybrid diagnosis method for inverter open-circuit faults in PMSM drives." *CES Transactions on Electrical Machines and Systems*, vol.4, no.3, pp.180-189, 2020.
- [22] C. Yongqi, and al. "Open-circuit fault diagnosis of traction inverter based on compressed sensing theory." *Chinese Journal of Electrical Engineering*, vol.6, no.1, pp.52-60, 2020.
- [23] R. Jyothi, and al. "Machine learning based multi class fault diagnosis tool for voltage source inverter driven induction motor." *Int J Pow Elec & Dri Syst*, vol.12.no.2, pp. 1205-1215, 2021.
- [24] H. Ran, R. Wang, and G. Zeng. "Fault Diagnosis Method of Power Electronic Converter Based on Broad Learning." *Complexity*, vol. 2020, 2020.
- [25] R. Abdelkader, and K. Abdelhafid. "Rolling bearing fault diagnosis based on improved complete ensemble empirical mode of decomposition with adaptive noise combined with minimum entropy deconvolution." *Journal of Vibroengineering*, vol.20, no.1, pp.240-257, 2018.
- [26] A. Rabah, et al. "Rolling bearing fault diagnosis based on an improved denoising method using the complete ensemble empirical mode decomposition and the optimized thresholding operation." *IEEE Sensors Journal*, vol.18, no.17, pp.7166-7172, 2018.
- [27] M. Fazel, G. A. Nazri, and M. Saif. "A fast fault detection and identification approach in power distribution systems." *2019 International Conference on Power Generation Systems and Renewable Energy Technologies (PGSRET)*. IEEE, 2019.
- [28] I. Miftah, and al. "Detection of the stator winding inter-turn faults in asynchronous and synchronous machines through the correlation between harmonics of the voltage of two magnetic flux sensors." *IEEE Transactions on Industry Applications*, vol.55, no.3, pp.2682-2689, 2019.
- [29] C. Bilal Djamel Eddine, A. Bendiabdellah, and M. Tabbakh. "An Automatic Diagnosis of an Inverter IGBT Open-Circuit Fault Based on HHT-ANN." *Electric Power Components and Systems*, vol.48, no.6-7, pp.589-602, 2020.
- [30] X. Yuqin, and al. "A method for diagnosing mechanical faults of on-load tap changer based on ensemble empirical mode decomposition, volterra model and decision acyclic graph support vector machine." *IEEE Access*, vol.7, pp.84803-84816, 2019.
- [31] H. Fouzi, and al. "An unsupervised monitoring procedure for detecting anomalies in photovoltaic systems using a one-class Support Vector Machine." *Solar Energy*, vol.179, pp.48-58, 2019.
- [32] A. M. Zawad, and al. "Machine learning-based fault diagnosis for single-and multi-faults in induction motors using measured stator currents and vibration signals." *IEEE Transactions on Industry Applications*, vol.55, no.3, pp.2378-2391, 2019.
- [33] A. M. Zawad, and al. "Machine learning based fault diagnosis for single-and multi-faults for induction motors fed by variable frequency drives." *2019 IEEE Industry Applications Society Annual Meeting*. IEEE, 2019.

[34] H. Wei, and al. "A Naive-Bayes-based fault diagnosis approach for analog circuit by using image-oriented feature extraction and selection technique." *IEEE Access*, vol.8, pp.5065-5079, 2019.

[35] J. M. Hatta, et al. "K-nearest neighbor and naïve Bayes based diagnostic analytic of harmonic source identification." *Bulletin of Electrical Engineering and Informatics*, vol.9, no.6, pp.2650-2657, 2020.

[36] S. Maciej, and al. "Effectiveness of selected neural network structures based on axial flux analysis in stator and rotor winding incipient fault detection of inverter-fed induction motors." *Energies*, vol.12, no.12, pp.2392, 2019.

[37] H. D. Tang, and H. J. Kang. "A motor current signal-based bearing fault diagnosis using deep learning and information fusion." *IEEE Transactions on Instrumentation and Measurement*, vol.69, no.6, pp.3325-3333, 2019.

[38] L. Chuang, and al. "Knowledge-based and data-driven approach based fault diagnosis for power-electronics energy conversion system." *2019 IEEE International Conference on Communications, Control, and Computing Technologies for Smart Grids (SmartGridComm)*. IEEE, 2019.

[39] Ü. Ramazan. "An Assessment of Imbalanced Control Chart Pattern Recognition by Artificial Neural Networks." *Artificial Intelligence and Machine Learning Applications in Civil, Mechanical, and Industrial Engineering*. IGI Global, pp.240-258, 2020.

[40] M. Feurer, and F.Hutter. "Hyperparameter optimization." *In Automated machine learning*, Springer, pp.3-33, 2019.

[41] M. Chouai, M. Merah, J. L. Sancho-Gomez, and M. Mimi. "Comparative study of supervised machine learning color-based segmentation for object detection in X-Ray baggage images for intelligent transportation systems." *In Emerging Trends in ICT for Sustainable Development*, Springer, pp. 89-98, 2021.

[42] H. Zhang. "The optimality of Naïve Bayes." *Seventeenth International Florida Artificial Intelligence Research Society Conference (FLAIRS)*, 2004.



Bilal Djamel Eddine Cherif received his Engineering degree from the University of M'sila, Algeria in 2010, his Magister Degree, and his Ph.D. degree in Electrical Engineering from the University of Sciences and Technology of Oran (USTO-MB), Algeria in 2015 and 2019. He is currently a Professor

Lecturer and researcher in the Electrical Engineering department, Faculty of Technology at the University of M'sila Algeria. His research interests include: electrical machines and drives modeling and analysis, electrical machines and drives control and converters as well as electrical machines and drives faults diagnosis and tolerance and machine learning.



Mohamed Chouai obtained his bachelor's degree in Automation and Control in Industries (2014), his master's degree in industrial computing (2016), and his Ph.D. in Signals, Systems Conception and their Applications from the University of Mostaganem, Algeria, for the development of systems based on machine / deep learning

technology and image processing (2020). His research interests include: Machine / Deep Learning, Image Processing, Video Processing, Pattern Recognition, Computer Vision, and Object Recognition.



Sara Seninete received her bachelor's degree in Electrical Engineering (2014), her Master's Degree in Industrial Computing and embedded systems (2016), and her Ph.D. degree in Signals, Systems Conception, and their Applications (2021) from the University of Mostaganem, Algeria. Her research

interests include: signal processing, machine learning, electrical machines and drives modeling and analysis, electrical machines and drives control and converters as well as electrical machines and drives faults diagnosis and tolerance.



Azeddine Bendiabdellah received his Bachelor of Engineering degree with honors and his Ph.D. degree from the University of Sheffield, England, in 1980, and 1985 respectively. From 1990 to 1991 he was a visiting professor at Tokyo Institute of Technology (T.I.T), Japan. He is currently a Professor

lecturer and researcher in the Electrical Engineering Faculty at the University of Sciences and Technology of Oran, (USTO-MB) Algeria. His research interests include: electrical machines and drives modeling and analysis, electrical machines and drives control and converters as well as electrical machines and drives faults diagnosis and tolerance.